# PROCEEDINGS OF SPIE

SPIEDigitalLibrary.org/conference-proceedings-of-spie

# Supporting Parker Solar Probe mission with Goode Solar Telescope at Big Bear Solar Observatory

Wenda Cao, Vasyl Yurchyshyn, Xu Yang, Kyung-Suk Cho, Haimin Wang

Wenda Cao, Vasyl Yurchyshyn, Xu Yang, Kyung-Suk Cho, Haimin Wang, "Supporting Parker Solar Probe mission with Goode Solar Telescope at Big Bear Solar Observatory," Proc. SPIE 12184, Ground-based and Airborne Instrumentation for Astronomy IX, 1218428 (29 August 2022); doi: 10.1117/12.2628741



Event: SPIE Astronomical Telescopes + Instrumentation, 2022, Montréal, Québec, Canada

# Supporting Parker Solar Probe Mission with Goode Solar Telescope at Big Bear Solar Observatory

Wenda Cao\*a,b, Vasyl Yurchyshyna,b, Xu Yanga,b, Kyung-Suk Choc,d, Haimin Wanga,b

<sup>a</sup>Big Bear Solar Observatory, New Jersey Institute of Technology, Big Bear City, CA, USA 92314; <sup>b</sup>Center for Solar-Terrestrial Research, New Jersey Institute of Technology, 323 Martin Luther King Boulevard, Newark, NJ, USA 07102; <sup>c</sup>Korea Astronomy and Space Science Institute, 776 Daedeokdaero, Yuseong-gu, Daejeon, Republic of Korea 34055; <sup>d</sup>Department of Astronomy and Space Science, University of Science and Technology, Daejeon, Republic of Korea 305-348

# **ABSTRACT**

New Jersey Institute of Technology (NJIT) has built, and now operates the 1.6-meter Goode Solar Telescope (GST) at the Big Bear Solar Observatory (BBSO), which was the highest-resolution solar telescope built in the U.S. in a generation. GST observations have been put in a campaign mode to support the NASA Parker Solar Probe (PSP) mission during its perihelia in 2019, 2020, 2021 and 2022, by providing unique high-resolution observations and critically complementary information on the photosphere and chromosphere at the source regions of solar wind acceleration and heating of solar corona. This paper presents the acquisition, processing, and archiving of high-resolution imaging spectroscopy and polarimetry data generated with GST instruments, as well as the preliminary scientific results.

**Keywords:** Solar telescope, high-resolution observation, spectrometer, spectropolarimeter, Parker Solar Probe (PSP)

## 1. INTRODUCTION

Fundamental discoveries in the field of heliophysics rely on advances of scientific instrumentation. This includes the tools that measure physical parameters in situ in a harsh environment, thus opening new energy domains, and advancing the state of the art in the spatial resolution and temporal cadence. The most exciting example is the NASA's Parker Solar Probe (PSP) mission, which is the first space mission to probe the innermost heliosphere, the closest accessible solar region, to determine the structure and dynamics of the Sun's coronal magnetic field, understand how the solar corona and wind are heated and accelerated, and determine what mechanisms accelerate and transport energetic particles (Bale et al. 2016; Fox et al. 2016; Kasper et al. 2016; McComas et al. 2016). This mission drives extended heliosphere observing campaigns, thus offering a unique opportunity for coordination in a way we have never done before. The coordination with other ground- and space-based assets is expected to enable an enhanced science return.

New Jersey Institute of Technology (NJIT) has built, and now operates one of the largest aperture ground-based solar telescopes in the world – the 1.6-meter Goode Solar Telescope (GST, Goode & Cao, 2012) at the Big Bear Solar Observatory (BBSO), California. GST, formerly known as the New Solar Telescope (NST), was the highest resolution solar telescope built in the U.S. in a generation. Benefitting from long periods of excellent local seeing at the Big Bear Lake, GST equipped with high-order adaptive optics, routinely collects diffraction-limited spatial resolution ( $\sim 0.1''$ ) photometric, spectroscopic and/or polarimetric data, with a high cadence (< 40 s), across the spectrum from 0.4 - 5.0  $\mu$ m. Since the beginning of its regular operation in 2010, GST has provided the community with open access to observations of the photosphere, chromosphere and up to the base of the corona with the unprecedented resolution, targeting at the fundamental nature of solar activity and the origin of space weather.

BBSO has a long history of supporting NASA space missions that date back to the first U.S. space station – the Skylab mission. Since then, BBSO has actively developed requisite instrumentation to provide unique complementary and supplementary support to various NASA space, rocket, and balloon missions. GST has routinely operated in campaigns with NASA *Hinode* and *IRIS* missions by targeting the same observing regions or solar events and offering the highest-resolution spectroscopy and spectro-polarimetry measurements of the solar atmosphere.

GST has been operated in a campaign mode in support of NASA PSP mission during its perihelia in 2019, 2020, 2021 and 2022, by providing critical complementary information on the photosphere and chromosphere at the source regions of solar wind acceleration and heating of the solar corona. The most relevant scientific contributions to the PSP

\*Correspondence: wenda.cao@njit.edu; phone 1 973 596-5301; fax 1 909 866-4240; www.bbso.njit.edu

Ground-based and Airborne Instrumentation for Astronomy IX, edited by Christopher J. Evans, Julia J. Bryant, Kentaro Motohara, Proc. of SPIE Vol. 12184, 1218428 © 2022 SPIE · 0277-786X · doi: 10.1117/12.2628741

science include studies of individual events such as coronal hole (CH) jets, as well as statistical investigation of small-scale magnetic reconnections, which are essential for understanding the energy and mass supply for coronal heating, solar flares, and solar wind acceleration. Our effort include acquisition, processing, and archiving of high-resolution imaging spectroscopy and polarimetry data generated with the GST requisite instruments. We have optimized the existing BBSO Data Processing/Pipeline System to generate level 0, level 1, and level 2 dataset in compliance with the NASA Solar Data Analysis Center (SDAC)'s requirement. All the data and metadata were made available to PSP users and the science community via the BBSO website (<a href="http://www.bbso.njit.edu/~vayur/gst\_logs/">http://www.bbso.njit.edu/~vayur/gst\_logs/</a>).

# 2. SCIENTIFIC MOTIVATION

PSP mission has three detailed scientific objectives (<a href="http://parkersolarprobe.jhuapl.edu/The-Mission/index.php#Science-Objectives">http://parkersolarprobe.jhuapl.edu/The-Mission/index.php#Science-Objectives</a>): (1) Trace the flow of energy that heats and accelerates the solar corona and solar wind; (2) Determine the structure and dynamics of the plasma and magnetic fields at the sources of the solar wind; (3) Explore mechanisms that accelerate and transport energetic particles. BBSO/GST aims at providing unique observations to reveal important information on the photosphere and chromosphere at the source regions of solar wind acceleration and heating of solar corona. These include vector magnetic field measurements with imaging spectro-polarimetry in the Fe I 1565 nm, and atmospheric dynamics as observed with the imaging spectroscopy in the white-light, Hα, Ca II 854.2 nm and He I 1083 nm (see details in Section 4). Here are three specific BBSO/GST observing projects that contribute the PSP science goals.

# 2.1 Jets in Coronal Holes (CHs)

Corona jets, especially those occurring in solar CHs can give rise to substantial disturbances in the solar wind, even though they are small and transient in nature. Roberts et al. (2018) simulated coronal jets encounters with PSP. They found that the jet front exhibits characteristics of a fast switch-on MHD shock, whose arrival is signaled by the sudden onset of large-amplitude transverse velocity and magnetic field oscillations. They also estimated that PSP will encounter numerous CH jets over the lifetime of the mission. Therefore, it is important to further our understanding of the origin and evolution of these small-scale jets with advanced observations of GST.

In previous studies, small-scale jets were well observed with GST in the regions such as sunspot light bridges (Tian et al. 2018). Those observing programs can be easily adapted for CH regions to obtain magnetograms, and  $H\alpha$  line-center and offband time sequence images. Figure 1 shows "Y" shaped jets that are likely due to reconnection between a small-scale emerging dipole and large-scale open fields extending to solar wind.

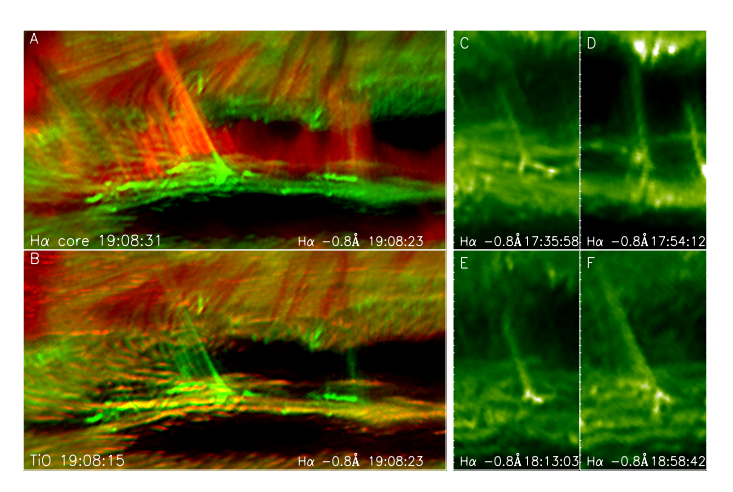


Figure 1: GST images of a light bridge with jets observed near the west limb on Oct 29, 2014. The small panels on the right feature inverted "Y" shaped jets which are considered to be manifestation of a reconnection process between a small-scale emerging dipole and inclined large-scale fields. (Courtesy of Tian et al. 2018)

#### 2.2 Statistical Analysis of Energy and Mass Output for Coronal Heating and Solar Wind

With the GST's unprecedented combination of spatial, spectral and temporal resolution, the chromosphere appears again to be a new frontier with the potential for new and significant findings. Although it is not possible to have one-to-one linkage between small-scale events and the solar wind features observed by PSP, a statistical analysis of energy release, mass transport as well as magnetic reconnection of small scales are highly relevant to PSP science goals and reflected in the corona/solar wind variation as probed by PSP. We list some examples of the contribution of our observations.

Type II spicules may be responsible for coronal heating and solar wind acceleration. These ejections are subject to various high frequency oscillations (Yurchyshyn et al. 2012; Sekse et al. 2013a, b; Srivastava et al. 2017; Yurchyshyn et al. 2020). Although it is not clear what drives these oscillations, two energy sources may be considered: p-mode leakage or magnetic tension release as suggested by Martinez-Sykora et al. (2017).

GST data will help to reveal the physics of type II spicules. The combination of high cadence (2 sec) chromospheric (H $\alpha$ ) imaging with GST imaging spectro-polarimetric measurements is both unique and critical to understand their energy release and transport in corona and solar wind.

Thanks to implementation of GST new generation adaptive optics, we significantly improved the sensitivity of magnetogram in the Quiet Sun (QS), as shown in Figure 2. We are developing advanced machine learning techniques to identify and trace evolution of magnetic elements, therefore their cancellation can be identified and correlated with occurrence of type II spicules. The energy released during these flux cancellation events will be estimated and compared to the energy released in typical spicules, giving a potential contribution to coronal heating.

Finally, high-resolution GST images of coronal loops at low temperatures provide a new and unrivaled method for observing the connection between chromospheric activity and heating of the corona. Ji, Cao & Goode (2012) found that coronal loops of diameter as small as 100 km, observed in the He I 1083 nm could be traced down to the locations of the photospheric concentrations. The past solar minimum during PSP encounter periods has offered a good chance to focus GST observations on the CH/QS and the associated coronal loops (see also Sahin et al. 2019). In particular, GST instruments are uniquely suited to investigate the evolution of magnetic footpoints of the loops rooted in the inter-granular lanes, as demonstrated by the results published in *Science* (Samanta et al. 2019).

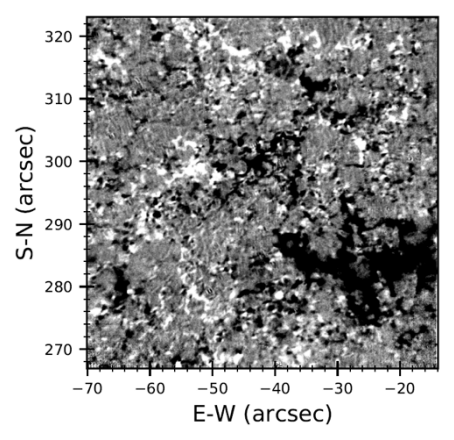
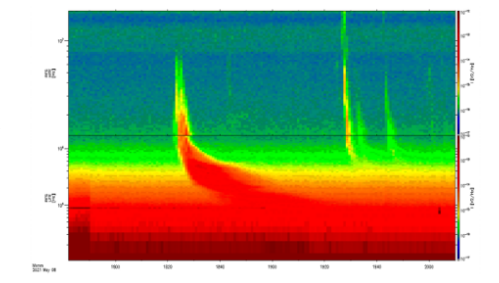


Figure 2: Unprecedentedly sensitive measurements of the quiet Sun line-of-sight magnetic fields obtained on June 7, 2018.

# 2.3 Study of Magnetic Reconnection Leading to Solar Flares and Electron Acceleration

It is anticipated that the solar activity level will increase in the coming years. GST can target the regions of magnetic reconnection and the associated sites of electron acceleration. Figure 3 shows feasibility of this study by comparing the GST observed evolution of flare ribbon front with the generated type III bursts as observed with the FIELDS/PSP. The rate of magnetic reconnection can be calculated from the ribbon separation speed and the measured magnetic field strength, in the same way was carried out for earlier studies (Qiu et al. 2002; Jing et al. 2005). We will explain



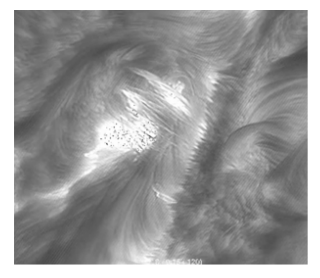


Figure 3: Left panel - type III bursts as observed by PSP/FIELDS on May 8, 2021, multiple peaks of electron acceleration is prominent. Right panel - GST Ha observation of the corresponding flare, showing fine structure of flare ribbon and loops. (Courtesy of FIELDS team)

temporally resolved electron accelerations observed by PSP with spatially resolved GST observation. In addition, hard X-ray observation from STIX on board Solar Orbiter will provide imaging for flare emissions.

### 3. GST AND KEY FOCAL PLANE INSTRUMENTATION

GST is an off-axis 1.6-meter clear aperture telescope that offers a significant improvement in ground-based, high spatial resolution and polarimetric capabilities (Goode & Cao 2012; Cao et al. 2010a, and also see the BBSO website at <a href="http://www.bbso.njit.edu/">http://www.bbso.njit.edu/</a>). Figure 4 shows a cutaway of the telescope system. Currently, the GST has six operational facility-class instruments (Cao et al. 2010a), including <a href="https://www.bbso.njit.edu/">BFI</a> (Broad-band Filter Imager), <a href="https://www.bbso.njit.edu/">VIS</a> (Visible Imaging Spectrometer), <a href="https://www.bbso.njit.edu/">NIRIS</a> (Near-InfraRed Imaging Spectropolarimeter), <a href="https://www.bbso.njit.edu/">FISS</a> (Fast Imaging Solar Spectrograph), <a href="https://www.bbso.njit.edu/">CYRA</a> (Cryogenic Solar Spectrograph), and <a href="https://www.bbso.njit.edu/">MIRIS</a> (NASA Mid-IR Imager). Operated simultaneously in most cases, the former four are in the <a href="https://www.bbso.njit.edu/">Coudé</a> Lab and are fed by light corrected by a high-order <a href="https://www.bbso.njit.edu/">AO/mCAO</a> (Adaptive Optics/Multi-Conjugate AO). <a href="https://www.bbso.njit.edu/">CYRA</a> resides on the floor above in its "clean room" and a grand piano sized cryostat. These facility-class imaging spectrometers and spectropolarimeters cover a wide spectrum of 430 nm - 5 \(mu\)m, from the shortest visible to the mid infrared. Many important solar spectral lines/molecular bands within this region can be observed photometrically, and/or spectroscopically and/or polarimetrically. All those scientific instruments are currently in daily operation and some of them have been used in support of the PSP mission.

BBSO lake-site is characterized by steady, AO correctable seeing all day long for more than half of each year (Hill et al. 2004; Kellerer et al. 2012). GST is the only large aperture solar telescope that has continuously stable observations lasting several hours daily. Thanks to unique AO correctable seeing at BBSO all day long and day after day, GST is ideal for campaigns and can work in coordination with the PSP observations. AO-equipped GST has achieved nearly diffraction-limited observations at a spatial resolution below 0.1", which are ideal for the study of small-scale physical processes in the photosphere and chromosphere (Goode et al. 2010; Yurchyshyn et al. 2011). Currently operating AO system at GST is the AO-308 system with 349 actuators (Shumko et al. 2014). AO-308 system provides diffraction-limited imaging even for raw, not speckle reconstructed data inside the isoplanatic patch. A data set is considered to be of good, scientific quality, when the isoplanatic patch is as large as 25". We have made a significant breakthrough in the MCAO pathfinder - Clear on the GST (Schmidt et al. 2017). Clear is not only today's most powerful solar MCAO system, but also currently the only MCAO system installed on a telescope and ready to look at the Sun. The basic system features three deformable mirrors, each with 357 actuators. Various wavefront sensor options are available with up to 208 sub-apertures, and up to a field of view (FOV) of 80" in the infrared. Clear expands the GST's diffraction limited FOV to cover entire active regions enabling critical spectroscopic and polarimetric observations.

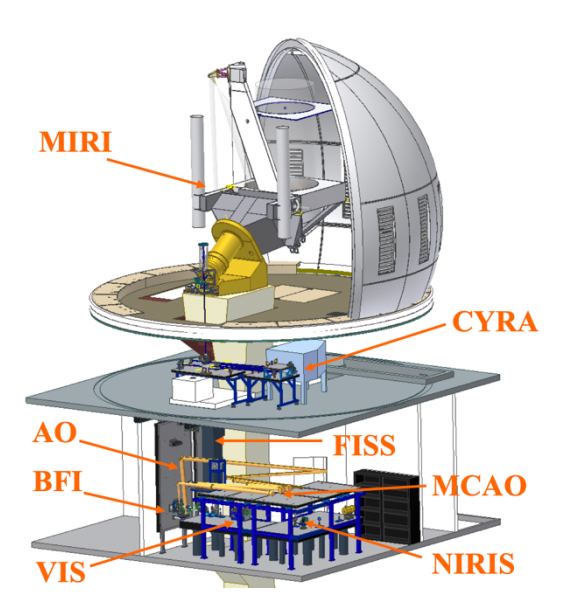


Figure 4: A schematic of the off-axis GST with its secondary mirror at the highest point. In the Coudé Lab, all light is first corrected by AO, then the beam is split into IR and visible light components, which are fed to GST scientific instruments (http://www.bbso.njit.edu/).

# 4. GST DATA IN SUPPORT OF PSP MISSION

Four GST science instruments are dedicated to support the PSP mission and Table 1 lists their detailed specifications and estimated data size to offer.

**Broadband Filter Imager (BFI):** On majority of days, imaging observations of the photosphere are performed with BFI (Cao et al. 2010b) by using a broadband TiO filter centered at a wavelength of 705.7 nm. This molecular band is sensitive to relatively cooler temperature, and thus well suited to observe the sunspot umbra/penumbra, granules/intergranular lanes. Another option is to use a G-band filter, which offers some advantages when observing the photospheric magnetic bright points. The FOV of the BFI is 77" by 77" with a pixel scale of 0".0375. This pixel size is 2.4 times smaller than the smallest resolved feature of GST ( $\theta = 1.03\lambda/D = 0$ ".09 ~ 65 km).

BFI data are acquired with a 2048 by 2048 PCO-2000 camera as bursts of 100 images each. Typical cadence ranges between 10-15 secs, depending on the observing target. Each burst is analyzed on the fly and the burst size is then reduced to 70 best contrast images, which are saved in the archive as a FITS file (level 0) with a total size of 560 MB.

BFI data processing consists of two steps: 1) Flat fielding of the entire burst, selecting the best contrast image out of 70 images in the burst and placing that image into the archive as a FITS file (level 1); and 2) Speckle reconstruction of each burst, which results in one single processed image (level 1.5) with enhanced contrast of the photospheric features.

We use the KISIP-7 software package developed by the Kiepenheuer Institute for Solar Physics, for speckle interferometry of GST AO-corrected solar imaging data (Wöger et al. 2008). It is a post AO reconstruction algorithm allowing to achieve the diffraction-limit. The code has been written in C programming language and optimized for parallel processing. The described processing pipeline is automatic and has been fully implemented for seven parallel computers at BBSO.

Typical observing day lasts for about 6 hours during which we may acquire up to 2160 bursts resulting in 1.18 TB level 0 data and about 17 GB of level 1 and 17 GB of speckle reconstructed (level 1.5) data. The level 1 or 1.5 data is a sequence of uncalibrated images, whose intensity is represented in digital number (DN) of the used camera.

<u>Visible Imaging Spectrometer (VIS):</u> VIS is an Fabry-Pérot-Interferometer-based tunable filter system, allowing us to performed imaging spectroscopy in H $\alpha$  (Cao et al. 2010a). It has a narrow bandpass of 0.08 Å and the possibility to shift its bandpass by 2 Å around the H $\alpha$  line center. The pixel scale is 0".029. A full line scan with a 0.2 Å step (13 predefined

positions) can be performed with a cadence of about 25 sec (or less, if no speckle reconstruction is planned). Images at one wavelength position can be taken with a much higher cadence of about 2 sec. The FOV of VIS is 74" by 63".

VIS operates in two modes: the first, and most used mode is the off-band scan imaging when a burst of 25 images (that parameter can be adjusted) is acquired at one or several predefined line positions (i.e.,  $\pm 1.2$  Å,  $\pm 1.0$  Å,  $\pm 0.8$  Å,  $\pm 0.6$  Å,  $\pm 0.4$  Å,  $\pm 0.2$  Å, and 0.0 Å from the H $\alpha$  line center). Further processing of the VIS burst is identical to the BFI data processing described above; the other mode is imaging spectroscopy, which allows an observer to rapidly scan a 4 Å (or smaller) spectral range with an arbitrary step, in this case no speckle reconstruction is performed since only one image is collected at one wavelength position. This mode is preferable when time cadence and spectral information are of paramount importance, although the spatial resolution is sacrificed.

Full observing day of 6 hours may generate up to 10800 bursts resulting in 2.78 TB of raw (level 0) data and about 111 GB of level 1 and 111 GB of speckle reconstructed (level 1.5) data. The level 1 or 1.5 data is a sequence of uncalibrated images, whose intensity is represented in digital number (DN) of the used camera.

Instru.	Measurement Characteristics	Maximum Date Size Level 0, 1, 2 (GB/day)	Best Cadence	Interest of Spectrum	Resolution	FOV	
BFI	Broadband Photometry imaging	L0: 1181; L1: 17; L1.5: 17	10 sec	TiO 705.7 nm or G-band 430.5 nm	< 0.1" with AO and speckle reconstruction	77"×77"	
VIS	Imaging spectroscopy	L0: 2781; L1: 111; L1.5: 111	3 sec	Нα	< 0.1" with AO and speckle reconstruction	74"×63"	
NIRIS	Imaging polarimetry	L0: 1680; L1: 275; L2: 14	45 sec	Fe I 1565 nm	0.2": Fe I polarimetry	85" (Round)	
	Imaging spectroscopy	L0: 1207; L1: 30; L1.5: 30	2 sec	He I 1083 nm	0.14": He I spectroscopy		
FISS	Imaging spectroscopy	L0: 60; L1: 60; L2: 60	90 sec	Hα 656.3 nm Ca II 854.2 nm	0.1" - $0.2$ " with AO $R_0 = \lambda/\Delta\lambda > 10^5$	40"×60"	

Table 1: GST Instruments in Support of PSP Mission and their Specifications.

Near InfraRed Imaging Spectropolarimeter (NIRIS): NIRIS (Cao et al. 2012; Ahn & Cao, 2016) produces unprecedented high-quality and high-sensitivity vector magnetic field measurements in the solar atmosphere. The primary lines of interests are the Fe I doublet at 1564.85 nm ( $g_{eff} = 3$ ) and 1565.29 nm ( $g_{eff} = 1.53$ ), which is the most Zeeman sensitive probe of the magnetic field in the deepest photosphere (~40 km below the level at which photons at 500 nm escape). The FOV of NIRIS is 85" in round shape, with a pixel scale of 0".083/pixel. This dual Fabry-Pérot system performs a line sampling of 60 points within 45 seconds. NIRIS can detect magnetic signals as low as 4 Gauss and can be accurate down to 10 Gauss for longitudinal magnetic field signals. A typical scan of 60 wavelength points generates 3.5 GB of raw data (level 0). The incoming polarized light is modulated by a rotating birefringent waveplate, so that the output intensity varies sinusoidally with a combination of different periods and phases. During data processing, we extract polarization signals by measuring the amplitudes of different modulation patterns (level 0). Because of strong instrumental polarization, we also measure the crosstalk of polarization signals introduced by the telescope and relay optics. It is done by using calibration optics that generates pure polarized lights, allowing us to measure the response of the optical systems at its terminal and remove the instrumental polarization effect from the collected data (level 1). The derived Stokes profiles are then inverted to deduce physical parameters of the magnetic fields. We use Milne-Eddington method and/or SIR inversion to generate the level 2 data.

In a typical observing day, NIRIS acquires 480 raw data files accounting for about 1.68 TB (level 0), which are calibrated into 275 GB of level 1 data and 14 GB of level 2 data. The level 1 data are intensity (in DN) images with the wavelength coordinate expressed in nm. The level 2 data are inverted maps of physical parameters, such as magnetic field strength map (in Gauss), magnetic field orientation map (azimuth angle and inclination, in degree), Doppler shift of the line center map (in nm), etc.

Alternately, NIRIS offers imaging spectroscopic data in the He I 1083 nm line, with a bandpass of 0.2 Å and an image scale of 0".063/pixel. Typically, NIRIS takes about 3 sec for an acquisition of a burst of 40 images at one wavelength. The spectroscopic observations are performed at the line center and  $\pm 0.2$ ,  $\pm 0.4$ ,  $\pm 0.6$ ,  $\pm 0.8$  Å off the He I line wing component. Further processing is identical to the VIS data processing described above. A full observing day of 6 hours generates up to 7000 bursts resulting in 1.2 TB of raw (level 0) data and about 30 GB of level 1 and 30 GB of speckle reconstructed (level 1.5) data. Those images are represented in DN of the used camera.

Fast Imaging Solar Spectrograph (FISS): FISS (Chae et al. 2013) is the visible to near-infrared spectrograph that scans the FOV by rapidly moving a set of two folding mirrors in front of the slit. It has a slit height of 40" and the scanning range can cover up to 60", which takes about 90 secs or less to complete. The spatial sampling is 0".16 per pixel after 2×1 binning. However, since FISS data are not speckle reconstructed, it yields a typical spatial resolution of about 0".5. Its desired spectral resolving power is  $1.4 \times 10^5$ . FISS has dual CCD cameras of  $512 \times 512$  pixels that can image two different bands simultaneously, thus enabling the use of multiple spectral line pairs, such as the Hα and Ca II 854.2 nm or Na D2 and Fe I 543.4 nm. When observing for 6 hours per day, it costs about 60 GB of the disk space. Once the raw data are taken, flat fields are acquired by moving the angle of diffraction grating in spectral direction (level 0). Additional processes are done to remove any horizontal lines due to dust on the slit, and correction of curvature in spectral lines on a 2D spectral images (level 1). The calibration of wavelength scale is performed to calculate line broadening, line width, and Doppler shift, so that the maps of physical parameters such as temperature maps (in Kelvin) and velocity maps (in m/s) would be provided (level 2).

# 5. SPECIAL EFFORT IN COMPLIANCE WITH PSP SCIENTIFIC REQUIREMENT

Although the routine observations and data processing are covered by BBSO operation, substantial effort has been made to ensure that the data are of satisfactory quality and can be easily used by PSP users and the science community to enhance the PSP science return. We focus on the following four aspects of observations and data processing.

### 5.1 GST Absolute Pointing and Accurate Alignment with Satellite Data

Unlike the space-based observations, the ground-based data acquiring process suffers from frequent displacements of the target region within the FOV mainly due to varying seeing conditions. The problem becomes important when the FOV is narrow as it is the case with GST. Although the AO system and/or the tip-tilt mirror allow us to stabilize the live image, additional co-alignments are required to ensure the necessary accuracy for studying small-scale phenomena. Guider calibration is performed every day before observations using solar limb. However, pointing errors, stemming from telescope flexure near the meridian, accumulate during the day. This leads to a situation when the target region is the center of the FOV due to the tip tilt mirror corrections, but the pointing information written into the FITS header differs from the actual pointing. To alleviate the problem, we perform additional guider calibrations before and after crossing the central meridian. We propose the following enhancements to improve the quality of level 1.5 data. The enhancements will be carried out by the data provider as one-time effort. We provide data in FITS standard, where one image is saved in one FITS file. Some efforts have been made to improve the quality of the relevant metadata (fits header information) by supplying 1) accurate information on heliocentric coordinates of the center of an image, allowing effortless image co-alignment, and 2) image de-rotation angle to properly orient data along the solar axes. To achieve these, we have worked on data imaging data registration within each instrument. It is especially important when dealing with multi-wavelength measurements, such as spectro-polarimetry data. This task has been the most time-consuming since accurate co-alignment of the near limb QS (most likely) features with other available data (say, HMI continuum images) is not a trivial matter, especially for large data samples. Based on the scale-invariant feature transform method and the optical flow method, we have developed two different approaches and applied them to the data sets collected under good seeing conditions during the 2019-2021 PSP perihelia (Yang et al. 2022). We will continuously improve these two approaches to adopt data sets with fair seeing conditions. The upgraded codes will be used to process the GST data taken during the 2022-2023 PSP perihelia.

# 5.2 Improve Stokes Inversion Algorithm with Machine Learning

When performing NIRIS data inversion from level 2 to level 3, one problem is that the existing inversion tools are either unable to deal with complex Stokes profiles (*i.e.*, asymmetrical and multi-lobed) or too slow (inversion of one magnetogram requires manual intervention and tens of PC hours) or both. We have begun exploring the use of machine-learning (ML) to the Stokes inversion of NIRIS data. Liu et al. (2020) have made such an effort based on a convolutional neural network (CNN) and the Milne-Eddington (ME) method. By learning the latent patterns in the training data prepared by the physics-based ME tool, the proposed CNN method can infer vector magnetic fields from the Stokes profiles of NIRIS. Experimental results show that our CNN method produces smoother and cleaner vector magnetic fields maps than the widely used ME method. Further, the CNN method is four to six times faster than the ME method and can produce vector magnetic fields in nearly real-time. The advanced ML methods allow us extract full and accurate information from observed Stokes profiles, significantly advancing our studies of small-scale magnetic fields and the role they play in coronal heating.

# 5.3 Drive Velocity Fields from H $\alpha$ and He I 1083 nm Imaging Spectroscopy

GST provides imaging spectroscopy in H $\alpha$  and He I 1083 nm. We have obtained outstanding scientific results, such as the velocity of flare footpoints (Huang et al. 2019), and Counter-Streaming motions in filaments (Wang et al. 2018, Yang et al. 2019). Current data product in velocity field measurement are being improved to better support the PSP in CH observations that has a much smaller scale and lower speed. This is due to limited wavelength points and some asymmetry in instrument line profile. We will (1) develop special observation sequences with more wavelength coverage; (2) calibrate instrument transmission much more carefully; (3) improve inversion tools to ensure the most accurate velocity measurements. The level 2 of VIS and He I data for velocity fields will be generated with these additional data processing steps to be provided.

# 5.4 GST Data Preparation for SDAC and VSO

Each data set submitted to SDAC were supplied with proper documentation, including i) instrument description, ii) data processing routine, iii) metadata description, and iv) observing log, notes and comment. The documentation also has contact information of GST instrument PIs as well as list of papers based on GST data, so that researchers new to the data have an opportunity to learn how data may be used as well as to contact authors if needs.

GST data collected from each instrument are stored in the instrument subfolder of the corresponding calendar day. Processed and calibrated data as well as relevant metadata are stored in the lower-level folders of the instrument subfolder. Speckle reconstructed BFI, VIS and He I 1083 nm images are saved in FITS format, one image per FITS file. NIRIS data are stored as a 4D FITS file per scan which include spatial coordinate (x, y), wavelength, and Stokes parameters. FISS data are also stored as in FITS format, one raster scan (x, y, and wavelength) per file.

GST instruments are expected to operate in their best cadences if seeing condition and local weather permit. In Table 1, we estimate the maximum data sizes that GST can generate under the best cadences. The raw data accounts for over 90% of the whole volumes. If needed, all raw data can be optionally compressed during their acquisition using the NASA HEASARC library with a lossless algorithm. The compression ratio ranges from 1.6 to 2.2.

Currently, all GST-PSP data have been archived at BBSO, which can be requested and downloaded via the BBSO website (<a href="http://www.bbso.njit.edu/~vayur/gst\_logs/">http://www.bbso.njit.edu/~vayur/gst\_logs/</a>). The properly documented data processed and enhanced as described above, will be submitted to SDAC for integration into the NASA data system. Moreover, together with VSO staff, we have designed and implemented a way to search and download BBSO full disk data using VSO capabilities. Similar protocol will apply to GST data.

# 6. ACCOMPLISHMENT HIGHLIGHTS

The spread of COVID-19 has significantly affected BBSO operations in 2020 and 2021. The observatory has been in lockdown several times following California-mandated stay-at-home order. In most cases, BBSO took action to have all staff work home as much as possible to mitigate the spread of the virus. When conditions and restrictions concerning COVID-19 were somewhat eased, BBSO started 'limited' operations in time to support the NASA PSP mission, when only one staff member was allowed to be present at the dome to operate the telescope. That individual operated solo for at least a few days before being relieved by another operator. BBSO did not resume its regular operation until California Governor terminated the stay-at-home order on June 15, 2021.

#### 6.1 GST Data Acquisition, Processing and Archiving

Despite these unexpected challenges, GST has successfully supported the NASA PSP mission during its perihelia in 2019, 2020, 2021 and 2022. All information on GST support of the NASA PSP mission is detailed in Table 2. GST has committed to continuously support PSP mission during the upcoming six perihelia in 2023 and 2024.

During the PSP perihelia, GST observing time has exclusively been reserved for supporting the PSP mission without accepting any external and internal observing proposals. The painstaking effort included acquiring, processing, and archiving high-resolution imaging spectroscopy and polarimetry data generated with GST requisite instruments – *BFI, VIS or FISS,* and *NIRIS.* When the PSP team (<a href="https://whpi.hao.ucar.edu/whpi\_campaign-cr2226.php">https://whpi.hao.ucar.edu/whpi\_campaign-cr2226.php</a>) provided the campaign targets (usually from consensus PSP footpoint prediction provided by Johns Hopkins University), GST was pointed at the suggested coordinates accordingly. Otherwise, GST duty scientists chose targets, primarily CHs or active regions (ARs). Specifically, CHs were assigned to be a priority GST target to obtain high-resolution imaging spectroscopy data in Hα, Ca II 854.2 nm, He I 1083 nm and vector magnetograms for 5-6 hours a day. We also observed the quiet sun in the photosphere near the disk center, to cover areas outside CHs, and to compare magnetic activity inside and outside CHs.

At this writing, a total of 360 GST observing days have been assigned for the PSP mission since the project started in 2019 during the PSP encounters #3 - #12. All these PSP supporting data have been processed and calibrated to level 1, level 1.5, or level 2. The processed data have been archived at BBSO and is openly available to all PSP users and the solar community via the BBSO website (<a href="http://www.bbso.njit.edu/~vayur/gst\_logs/">http://www.bbso.njit.edu/~vayur/gst\_logs/</a>). We are now coordinating with the NASA SDAC to transfer the data and requisite documentation to SDAC and make it available to the public via the Virtual Solar Observatory infrastructure.

Table 2: GST supporting NASA PSP mission in 2019, 2020, 2021, 2022 and 2023

Encounter	Perihelion Date	GST Observing Duration	<b>GST Instruments</b>	Observing Tasks	
#3	09/01/2019	08/02/2019 - 09/30/2019	BFI, VIS/FISS, NIRIS		
#4	01/29/2020	12/25/2019 - 02/28/2020	BFI, VIS/FISS, NIRIS		
#5	06/07/2020	05/08/2020 - 07/07/2020	BFI, VIS/FISS, NIRIS		
#6	09/27/2020	08/28/2020 - 10/27/2020	BFI, VIS/FISS, NIRIS		
#7	01/17/2021	01/04/2020 - 01/31/2021	BFI, VIS/FISS, NIRIS	Campaions with	
#8	04/29/2021	04/22/2021 - 05/07/2021	BFI, VIS/FISS, NIRIS		
#9	08/09/2021		BFI, VIS/FISS, NIRIS	1 51 1/11551011	
#10			BFI, VIS/FISS, NIRIS		
#11	02/25/2022	5/2022 02/14/2022 - 03/06/2022 BFI, VIS/FISS, NIRIS			
#12	06/01/2022	05/23/2022 - 06/11/2022	BFI, VIS/FISS, NIRIS		
#13	09/06/2022	08/27/2022 - 09/16/2022	BFI, VIS/FISS, NIRIS		
#14	12/11/2022	11/28/2022 - 12/23/2022	BFI, VIS/FISS, NIRIS		
#15	03/17/2023	03/03/2023 - 03/31/2023	BFI, VIS/FISS, NIRIS	Committed Observing	
#16	06/22/2023	06/13/2023 - 07/02/2023	BFI, VIS/FISS, NIRIS	Campaigns with PSP Mission	
#17	09/27/2023 09/18/2023 - 10/07/		BFI, VIS/FISS, NIRIS	1 51 1/11551011	
#18	12/29/2023	12/15/2023 - 01/12/2024	BFI, VIS/FISS, NIRIS		

# 6.2 Scientific Results

Lee et al. (2021) investigated high resolution  $H\alpha$  images and magnetograms obtained with GST to explore solar origin for the solar wind switchbacks. In this effort, the authors measured the spatial dimensions, the orientation, and the eruption speed of tiny magnetic arcades, mini-filaments, and plumelets to compare with the properties of switchbacks established from PSP observations. The spatial dimensions of these solar events range from tens of arcsecond down to sub arcseconds (200 km), small enough to produce short duration switchbacks in the solar wind. However, the orientation combined with the speed can be tested against the surprisingly high aspect ratio of the switchbacks, thus providing a strong constraint on the possible candidates. Other properties of the switchbacks, such as clustering and one-sidedness, make this search a narrower choice. The authors argue that the most ideal solar candidate should be a tiny upright flux tubes that can develop into an S-shape after ejection under some instability arising from the density inhomogeneity along the flux tube.

Huang et al. (2021) surveyed small-scale energetic events at and near the boundaries of CHs from the lower chromosphere to the corona. Full disk extreme ultraviolet (EUV) images and H $\alpha$  far bluewing images were used to identify the activities in the coronal and chromospheric activity, respectively. The authors compare the statistical distribution of their lifetimes and occurrence frequencies. Moreover, for the activities that are potentially related to switchbacks detected by PSP, they used high-resolution observations from GST and spectral data from IRIS to study their dynamic structures in detail and linkage to magnetic field evolution.

# **ACKNOWLEDGEMENT**

Big Bear Solar Observatory operation is supported by New Jersey Institute of Technology and US NSF AGS-1821294 grant. Goode Solar Telescope operation is partly supported by the Korea Astronomy and Space Science Institute and the Seoul National University. We acknowledge support from NASA grants - 80NSSC20K0025, 80NSSC21K1671 and

80NSSC20K1282, as well as US NSF grants - AGS-1821294 and AST-2108235. We thank Dr. Stuart Bale for preparing the plot of PSP/FIELDS data.

# REFERENCES

- [1] Bale, S. D.; Goetz, K.; Harvey, P. R., et al., "The FIELDS Instrument Suite for Solar Probe Plus. Measuring the Coronal Plasma and Magnetic Field, Plasma Waves and Turbulence, and Radio Signatures of Solar Transients", Space Sci. Rev., 204, 49 (2016).
- [2] Cao, W., Goode, P. R., Ahn, K., Gorceix, N., Schmidt, W., & Lin, H., "NIRIS the Second Generation Near-Infrared Imaging Spectro-polarimeter for the 1.6 meter off-axis New Solar Telescope", ASPC, 463, 291 (2012).
- [3] Cao, W., Gorceix, N., Coulter, R., Ahn, K., Rimmele, T. R., & Goode, P. R., "Scientific instrumentation for the 1.6-meter New Solar Telescope in Big Bear", Astronomische Nachrichten, 331, 636 (2010a).
- [4] Cao, W., Gorceix, N., Coulter, R., Coulter, A., K., & Goode, P. R., "First Light of the 1.6 meter off-axis New Solar Telescope at Big Bear Solar Observatory", Proc. SPIE, 7733, 773330 (2010b).
- [5] Chae, J., Park, H., Ahn, K., Yang, H., Park, Y., Nah, J., Jang, B., Cho, K., Cao, W., & Goode, P., "Fast Imaging Solar Spectrograph of the 1.6 Meter New Solar Telescope at Big Bear Solar Observatory", Solar Physics, 288, 1 (2013).
- [6] Fox, N. J.; Velli, M. C.; Bale, S. D., et al., "The Solar Probe Plus Mission: Humanity's First Visit to Our Star", Space Sci. Rev., 204, 7 (2016).
- [7] Goode, P. R. & Cao, W., 2012, "The 1.6 m Off-axis New Solar Telescope (NST) in Big Bear", Proc. SPIE, 8444, 844403 (2012).
- [8] Goode, P. R., Yurchyshyn, V., Cao, W., Abramenko, V., & Andic, A., "Highest Resolution Observations of the Quietest Sun", ApJ, 714, L31-L35 (2010).
- [9] Hill, F., Beckers, J., Brandt, P., et al., "Solar site testing for the Advanced Technology Solar Telescope", Proc. SPIE, 5489, 122 (2004).
- [10] Huang, Nengyi; Xu, Yan; Sadykov, Viacheslav M.; Jing, Ju & Wang, Haimin, "Spectral Diagnosis of Ma II and Ha Lines during the Initial Stage of an M6.5 Solar Flare", ApJ, 878, 15 (2019).
- [11] Huang, Nengyi; Yang, Xu; Lee, Jeongwoo; Yurchyshyn Vasyl; Cao, Wenda; Haimin Wang, "A Statistical Study of Small-Scale Energy Releases on the Sun as Possible Origins of Switchbacks", ApJ, under review (2022).
- [12] Ji, H., Cao, W. & Goode, P. R., "Observation of Ultrafine Channels of Solar Corona Heating", ApJ Lett., 750, L25 (2012).
- [13] Ju Jing, Jiong Qiu, Jun Lin, Ming Qu, Yan Xu, & Haimin Wang, "Magnetic Reconnection Rate and Flux-Rope Acceleration of Two-Ribbon Flares", ApJ, 620, 1085 (2005).
- [14] Kasper, Justin C.; Abiad, Robert; Austin, Gerry, et al., "Solar Wind Electrons Alphas and Protons (SWEAP) Investigation: Design of the Solar Wind and Coronal Plasma Instrument Suite for Solar Probe Plus", Space Sci. Rev., 204, 131 (2016).
- [15] Kellerer, A., Gorceix, N., Marino, J., Cao, W., & Goode, P. R., "Profiles of the Daytime Atmospheric Turbulence Above Big Bear Solar Observatory", A&A, 542, A2 (2012).
- [16] Lee, Jeongwoo; Yang, Xu; Yurchyshyn, Vasyl; Cao, Wenda; Wang, Haimin, "Solar Chromospheric Ejections and Solar Wind Switchbacks", ApJ, under review (2022).
- [17] Hao Liu, Yan Xu, Jiasheng Wang, Ju Jing, Chang Liu, Jason T. L. Wang, and Haimin Wang, "Inferring Vector Magnetic Fields from Stokes Profiles of GST/NIRIS Using a Convolutional Neural Network", ApJ, 894, 70 (2020).
- [18] Martínez-Sykora, J., De Pontieu, B., Hansteen, V. H., Rouppe van der Voort, L., Carlsson, M. & Pereira, T. M. D., "On the generation of solar spicules and Alfvénic waves", Science, 356, 6344, 1269 (2017).
- [19] McComas, D. J.; Alexander, N.; Angold, N., et al., "Integrated Science Investigation of the Sun (ISIS): Design of the Energetic Particle Investigation", Space Sci. Rev., 204, 187 (2016).
- [20] Qiu, J., Lee J., Gary, D., & Wang, H., "Motion of Flare Footpoint Emission and Inferred Electric Field in Reconnection Current Sheets", ApJ, 565, 1335 (2002).
- [21] Roberts, Merrill A., Uritsky, Vadim M., DeVore, C. Richard, & Karpen, Judith T., "Simulated Encounters of the Parker Solar Probe with a Coronal-hole Jet", ApJ, 866, 14 (2018).
- [22] Sahin, S., Yurchyshyn, V., Kumar, P., Kilcik, A., Ahn, K., & Yang, X., "Magnetic Field Dynamis and Varying Plasma Emission in Large-scale Coronal Loops", ApJ, 873, 75 (2019).

- [23] Samanta, T., Tian, H., Yurchyshyn, V., Peter, H., Cao, W., Sterling, A., Erdélyi, R., Ahn, K., Feng, S., Utz, D., Banerjee, D., & Chen, F., "Generation of Solar Spicules and Subsequent Atmospheric Heating", Science, 366, 890 (2019).
- [24] Schmidt, D., Gorceix, N., Goode, P. R., Marino, J., Rimmele, T., Berkefeld, T., Wöger, F., Zhang, X., Rigaut, F., & von der Lühe, O., "Clear widens the field for observations of the Sun with multi-conjugate adaptive optics", A&A, 597, L8 (2017).
- [25] Shumko, S., Gorceix, N., Choi, S., Kellerer, A., Cao, W., Goode, P. R., Abramenko, V., Richards, K., Rimmelle, T. R., & Marino, J., "AO-308: the High-order Adaptive Optics System at Big Bear Solar Observatory", Proc. SPIE, 9148, 35 (2014).
- [26] Sekse, D. H.; Rouppe van der Voort, L.; De Pontieu, B., "On the Temporal Evolution of the Disk Counterpart of Type II Spicules in the Quiet Sun", ApJ, 764, 164 (2013a)
- [27] Sekse, D. H.; Rouppe van der Voort, L.; De Pontieu, B.; Scullion, E., "Interplay of Three Kinds of Motion in the Disk Counterpart of Type II Spicules: Upflow, Transversal, and Torsional Motions", ApJ, 769, 44 (2013b).
- [28] Srivastava, A. K., Shetye, J., Murawski, K., Doyle, J. G., Stangalini, M., Scullion, E., Ray, T., Wójcik, D. P. & Dwivedi, B. N., "High-frequency torsional Alfvén waves as an energy source for coronal heating", Scientific Reports, 7, 43147 (2017).
- [29] Hui Tian, Vasyl Yurchyshyn, Hardi Peter, Sami K. Solanki, Peter R. Young, Lei Ni, Wenda Cao, Kaifan Ji, Yingjie Zhu, Jingwen Zhang, Tanmoy Samanta, Yongliang Song, Jiansen He, Linghua Wang, & Yajie Chen, "Frequently Occurring Reconnection Jets from Sunspot Light Bridges", ApJ, 854, 92 (2018).
- [30] Wang, Haimin; Liu, Rui; Li, Qin; Liu, Chang; Deng, Na; Xu, Yan; Jing, Ju; Wang, Yuming & Cao, Wenda, "Extending Counter-streaming Motion from an Active Region Filament to a Sunspot Light Bridge", ApJL, 852, 18 (2018).
- [31] Wöger, F., von der Lühe, O., & Reardon, K., "Speckle interferometry with adaptive optics corrected solar data", A&A, 488, 375 (2008).
- [32] Xu Yang, Wenda Cao, Haisheng Ji, Parida Hashim, & Jinhua Shen, "High-resolution Spectroscopic Imaging of Counter-streaming Motions in Solar Active Region Magnetic Loops", ApJL, 881, L25 (2019).
- [33] Xu Yang, Wenda Cao, & Vasyl Yurchyshyn, "GST Data Registration and Alignment Workflow", A&A, under review (2022).
- [34] Yurchyshyn, V., Ahn, K., Abramenko, V., Goode, P. & Cao, W., 2012, Small Scale Field Emergence and Its Impact on Photospheric Granulation, ArXiv e-prints, arXiv:1207.6418v (2012).
- [35] Yurchyshyn, V., Cao, W., Abramenko, V., Yang, X., & Cho, K.-S., "Rapid Evolution of Type II Spicules Observed in Goode Solar Telescope On-disk Ha Images", ApJL, 891, L21 (2020).
- [36] Yurchyshyn, V., Goode, P. R., Abramenko, V. I., Chae, J., Cao, W., Andic, A., & Ahn, K., "Chromospheric Signatures of Small-scale Flux Emergence as Observed with New Solar Telescope and Hinode Instruments", ApJ, 722, 1970 (2011).